Infrared Spectroscopy Studies of CH···O Hydrogen Bondings and Thermal Behavior of Biodegradable Poly(hydroxyalkanoate)

Harumi Sato,[†] Rumi Murakami,[†] Adchara Padermshoke,[†] Fuminobu Hirose,[‡] Kenichi Senda,[‡] Isao Noda,[§] and Yukihiro Ozaki*,[†]

Department of Chemistry, School of Science and Technology, Kwansei-Gakuin University, Sanda 669-1337, Japan; Polymer Designing and Processing Research Laboratories, Kaneka Corporation, Settsu 566-0072, Japan; and The Procter and Gamble Company, 8611 Beckett Road, West Chester, Ohio 45069

Received May 5, 2004; Revised Manuscript Received July 5, 2004

ABSTRACT: Infrared (IR) spectra of new types of bacterial copolyester, poly(3-hydroxybutyrate-*co*-3-hydroxyhexanoate), P(HB-*co*-HHx) (HHx = 2.5, 3.4, and 12 mol %), and poly(3-hydroxybutyrate) (PHB) were measured over a temperature range of 20 °C to higher temperatures (PHB, 185 °C; HHx = 2.5 mol %, 160 °C; HHx = 3.4 mol %, 160 °C; HHx = 12 mol %, 140 °C) to explore their structure and thermal behavior. The temperature-dependent IR spectral variations were analyzed for the CH stretching, C═O stretching, CH_3 deformation, and C−O−C stretching vibration regions, and bands characteristic of crystalline and amorphous parts were identified in each region. It has been found from the anomalous frequencies of the CH_3 asymmetric stretching bands of the four polymers and the X-ray crystallographic structure of PHB that there is an inter- or intramolecular interaction (C−H···O hydrogen bond) between the C═O group in one helical structure and the CH_3 group in the other helical structure in PHB and P(HB-*co*-HHx). The bonding energy of the C−H···O hydrogen bond seems to be smaller than 4 kJ/mol, but considering the heat of fusion (12.5 kJ/mol) of PHB, it is likely that a chain of C−H···O hydrogen bond pairs link two parallel helical structures in the crystalline parts. The temperature-dependent IR spectral variations have shown that the crystallinity of P(HB-*co*-HHx) (HHx = 12 mol %) decreases gradually from a fairly low temperature (about 60 °C), while the crystallinity of PHB and P(HB-*co*-HHx) (HHx = 2.5 and 3.4 mol %) remains almost unchanged until just below their melting temperatures. It has also been revealed from the present study that the weakening of the C−H···O interaction starts from just above room temperature and proceeds gradually with increase in temperature, but the collapse of helical structure occurs at a much higher temperature for all the polymers investigated.

Introduction

Recently, various biologically synthesized polyesters produced by microorganisms have been receiving keen interest as new environmentally friendly materials.[1−5] They are biodegradable under aerobic and anaerobic conditions and can be produced from renewable resources. Some of these naturally occurring polyesters are perfectly biocompatible, and thus not only their industrial applications but also medical applications are explored. Among all natural polymers, only poly(hydroxyalkanoate) (PHA) polymers possess thermoplasticity and mechanical properties similar to those of synthetic polymers.[6−9] Thus, many research groups have been involved in developing PHAs with desirable physical properties.

Poly(3-hydroxybutyrate) (PHB), the most abundant polyester found in bacteria, has similar thermal and mechanical properties to isotactic polypropylene (iPP).[7,10] PHB is rigid and stiff because of high crystallinity, being not necessarily well suited for certain applications as a commodity plastics. PHB is also thermally unstable during the conventional melt processing due to the high melt temperature. To reduce the excess crystallinity and improve the overall physical properties of PHB, other monomers are sometimes copolymerized with PHB.[9,11−13] The PHB-based copolymers show a wide range of physical properties depending on the chemical structure of the comonomer units as well as the comonomer composition.

Recently, the Procter and Gamble Co. (Cincinatti, OH) has introduced a broad new class of PHA copolymers with a small amount of medium length side groups, which has been commercialized under the trade name Nodax.[10] Kaneka Corp. (Osaka, Japan) succeeded for the first time in biologically producing the poly(3-hydroxybutyrate-*co*-3-hydroxyhexanoate) or P(HB-*co*-HHx) from oils and fats by Aeromonas sp.OL338 and Aeromonas Sp.FA440,[14,15] which is a stereoregular random copolymer of [*R*]-3-hydroxybutyrate and [*R*]-3-hydroxyhexanoate units. This class of copolymers demonstrate some attractive properties, for example, anaerobic and aerobic degradability, alkaline digestibility, hydrolytic stability, good odor and oxygen barrier, ideal surface properties for printability, and so on. It further shows substantially reduced crystallinity and increased flexibility compared to those of the PHB homopolymer.

Figure 1 compares chemical structures of PHB (A) and P(HB-*co*-HHx) (B). The biodegradation mechanism, chemical synthesis, and mechanical properties of P(HB-*co*-HHx) were studied by several research groups.[9,11−13] The thermal behavior of P(HB-*co*-HHx) was also investigated by differential scanning calorimetry (DSC)[9,11,13] and infrared (IR) spectroscopy.[16−19]

Furthermore, P(HB-*co*-HHx) has excellent compatibility with other biodegradable polymers and synthetic polymers.[10] P(HB-*co*-HHx) may find uses in a variety

[†] Kwansei Gakuin University.
[‡] Kaneka Corp.
[§] Procter and Gamble Co.
* To whom all correspondence should be addressed: e-mail ozaki@ksc.kwansei.ac.jp.

10.1021/ma049117o CCC: $27.50
Published on Web 08/25/2004

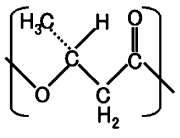

PHB

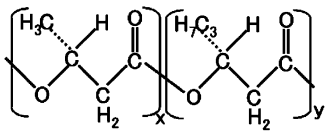

P(HB-*co*-HHx)
(HHx=2.5, 3.4, and 12 mol %)

Figure 1. Chemical structures of (A) poly(3-hydroxybutyrate) (PHB) and (B) poly(3-hydroxybutyrate-*co*-3-hydroxyhexanoate), (P(HB-*co*-HHx)) (HHx = 2.5, 3.4, and 12 mol %).

of polymer applications because it is possible to control the mechanical properties by changing the comonomer composition to produce forms ranging from fibers to films as well as molded plastic products. These new products are expected to be used not only for biodegradable polymers but also for medical materials because of their biocompatibility.

We have been investigating structure, crystallinity, and thermal behavior of PHB and P(HB-*co*-HHx) (HHx = 12 mol %) by using wide-angle X-ray diffraction (WAXD), IR spectroscopy, and differential scanning calorimetry (DSC).[20−22] WAXD is very useful not only as a tool to investigate a crystal structure but also as a method to explore thermally induced changes in the unit cell dimensions as a result of thermal expansion. IR spectroscopy is powerful to monitor temperature-dependent changes in the inter- and intramolecular interactions and conformations. Combination of WAXD, IR, and DSC is of particular importance to the study of structure and physical properties and their relations to the molecular construct of the polymers.

In the first paper of a series of our IR and WAXD studies on PHAs, we reported the results of the WAXD study of PHB and P(HB-*co*-HHx) (HHx = 12 mol %).[20] The WAXD pattern at room temperature showed that the P(HB-*co*-HHx) copolymer has an orthorhombic system ($\alpha = \beta = \gamma = 90°$) with $a = 5.76$ Å, $b = 13.20$ Å, and $c = 5.96$ Å (fiber repeat), which is identical to the crystal system of PHB homopolymer.[20] The WAXD study revealed that the thermal behavior of P(HB-*co*-HHx) is largely different from that of PHB. The (110) peak area of P(HB-*co*-HHx) starts decreasing from around 50 °C while that of PHB changes little at least until 140 °C, indicating that the crystallinity of PHB remains almost unchanged until 140 °C but that of P(HB-*co*-HHx) decreases gradually from fairly low temperature (∼50 °C).[20] Measurements of the *d* spacing from WAXD indicated a gradual expansion of the (110) *d* spacing of P(HB-*co*-HHx) and PHB lattice as temperature increases. The *a* lattice parameter shows the thermal expansion, while the *b* lattice parameter shows very little change for PHB and only a very slight change for P(HB-*co*-HHx). This result suggested that there is an inter- and intramolecular interaction between the C═O group and the CH_3 group in the P(HB-*co*-HHx) and PHB crystallites and that the interaction becomes weak with temperature along the *a* axis.[20] In the second paper we reported two-dimensional (2D) IR correlation spectroscopy study of PHB and P(HB-*co*-HHx) (HHx = 12 mol %).[22] This study suggested that melting of the crystalline structure does not simultaneously result in the formation of the completely amorphous structure. The phase transition process of PHB and P(HB-*co*-HHx) (HHx = 12 mol %) takes place through an intermediate state. It was noted in the 2D IR study that the vibrational frequencies of the C═O, C−O−C, and C−H stretching bands due to the crystalline components of P(HB-*co*-HHx) (HHx = 12 mol %) are almost identical with those of PHB. These observations indicated that the helical structure of P(HB-*co*-HHx) (HHx = 12 mol %) is very similar to that of PHB.

The purpose of the present study is to investigate the structure and thermal behavior of four kinds of PHAs, PHB, and P(HB-*co*-HHx) (HHx = 2.5, 3.5, and 12 mol %) by means of IR spectroscopy. The temperature-dependent IR spectra have been analyzed in detail in the C═O stretching, CH stretching, and C−O−C stretching vibration regions by using the second-derivative spectra and difference spectra. Particular attention has been paid to the following points: (1) the existence and thermally induced changes of the C−H···O hydrogen bond between the C═O group and the CH_3 group, (2) the relationship between the weakening of the C−H···O interaction and deformation of helical structure of PHAs, and (3) difference in the structure and thermal behavior among the four polymers. In other words, the effects of the inclusion of the HHx comonomer on the structure and thermal behavior were systematically studied. In recent years, C−H···O hydrogen bonding has received keen interest because of its potential capability for stabilizing particular structures of molecules and molecular interactions.[23−25] The present study should provide new insight into the C−H···O hydrogen bonding in the PHAs and reveal its role in combining the helical structures and in the thermal behavior of PHAs.

Experimental Section

Samples. Bacterially synthesized PHB and P(HB-*co*-HHx) (HHx = 12 mol %) were obtained from the Procter and Gamble Co., Cincinnati, OH. P(HB-*co*-HHx) (HHx = 2.5 and 3.5 mol %) were provided by Kaneka Co., Osaka, Japan. They were dissolved in hot chloroform, reprecipitated in methanol as fine powder, and vacuum-dried at 60 °C. Films of PHB and P(HB-*co*-HHx) (HHx = 2.5, 3.4, and 12 mol %) were prepared by casting their chloroform solutions on CaF_2 windows. The films were kept in a vacuum-dried oven at 60 °C for 12 h and cooled to room temperature.

IR Measurements. The transmission IR spectra were measured at a 2 cm^{-1} resolution using a Thermo Nicolet NEXUS 470 Fourier transform IR spectrometer with a liquid nitrogen cooled mercury−cadmium−telluride detector. A total of 512 scans were coadded for each IR spectral measurement to ensure a high signal-to-noise ratio. The temperature of the IR cell was controlled by a thermoelectric device (CN4400, OMEGA) with an accuracy of ±0.1 °C. The temperature was increased at a rate of ca. 2 °C/min. After changing the temperature, the cell was maintained at that temperature for 15 min to make the samples equilibrate.

Data Analysis. Data processing such as the calculation of second-derivative spectra was performed by program named SPINA 3.0 composed by Y. Katsumoto (Kwansei Gakuin University). The second derivatives were calculated using the Savizky−Golay method with the number of smoothing points being equal to 7.

Results and Discussion

Distance between the C═O Group and the CH_3 Group in PHB. To interpret the IR data of PHB and P(HB-*co*-HHx) (HHx = 2.5, 3.4, and 12 mol %), we have reexamined the structure of PHB elucidated by X-ray

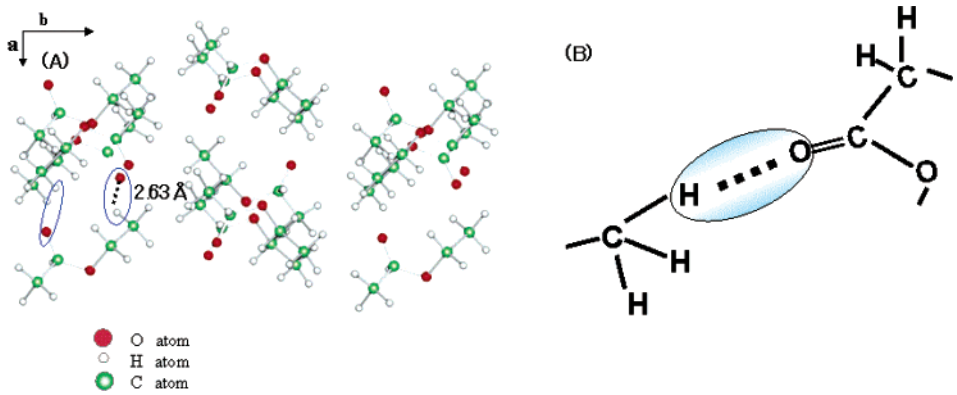

Figure 2. (A) Crystal structure of PHB calculated by the reported atom coordinates of PHB[15] by using the software QUANTA (Accelrys, San Diego, CA). (B) Distance between the H atom of one of the three C−H bonds of the CH_3 group and the O atom of the C═O group.

crystallographic studies.[26,27] In our previous paper on the WAXD studies of PHB and P(HB-*co*-HHx) (HHx = 12 mol %),[20] we reported that the C═O group in one helix and the CH_3 group in the other helix are located closely in the crystalline part, and there may be a C−H···O interaction between them. This time we calculated the distance between the O atom of the C═O group and the H atom of one of the C−H bonds of the CH_3 group from the reported atom coordinates of PHB[27] by using the software QUANTA (Accelrys, San Diego, CA). The atomic coordinates of PHB did not contain those for the H atoms. Therefore, in this calculation, we rotated the CH_3 group to look for the shortest distance between the H atom of the CH_3 group and the O atom of the C═O group. Figure 2A illustrates the crystalline structure of PHB, and the shortest distance was found to be 2.63 Å (Figure 2B). The van der Waals separation between the O atom and the H atom is 2.72 Å, and therefore, the distance between the O atom and the H atom in PHB can be significantly shorter than that of the van der Waals separation. The result of this calculation leads us to infer the existence of the C−H···O interaction in PHB. Our previous temperature-dependent WAXD study on PHB[20] and the results of IR spectra described later strongly support this possibility. It is very likely that a similar interaction exists in P(HB-*co*-HHx) (HHx = 2.5, 3.4, and 12 mol %).

C═O Stretching Band Region of IR Spectra. Figure 3 shows the temperature-dependent IR spectra in the C═O stretching band region of films of PHB and P(HB-*co*-HHx) (HHx = 2.5, 3.4, and 12 mol %). Their second derivatives are shown in each figure. Figure 4A−D illustrates the difference spectra calculated from the spectra shown in Figure 3A−D, respectively, using the spectra measured at room temperature as references.

The results of second derivatives and difference spectra reveal that there are three major bands in the C═O stretching band region. One is located at 1723 cm^{-1}. This band is intense at room temperature, but its intensity decreases with temperature and eventually disappears at high temperature (Figures 3 and 4). Thus, this band is very much characteristic of the crystalline form.[16−19,21,22] The other two bands are observed near 1750 and 1735 cm^{-1} (see the second-derivative spectra in Figure 3 and the difference spectra in Figure 4). It should be noted that a broad feature near 1740 cm^{-1} in the spectra shown in Figure 3 is not a single band but consists of two bands near 1750 and 1735 cm^{-1}. These bands are relatively weak in the spectra at room temperature, and their intensity increases with temperature. It can be seen also from Figure 3 that the relative intensities of the bands at 1750 and 1735 cm^{-1} increase largely with the increase in the HHx content. Judging from the frequencies and the temperature-dependent and HHx content-dependent variations, we assign the two bands at 1750 and 1735 cm^{-1} to the C═O stretching modes of amorphous parts. The quantum chemical calculations by Dybal et al.[28] indicate that the two C═O stretching bands arise from the different conformation of the main chain.

The crystalline C═O stretching band appears near 1723 cm^{-1}, which is lower by about 25 cm^{-1} compared with the frequency of the stretching band of a free ester C═O group. For the origin of this low-frequency shift there are three possibilities. One is the interaction between the C═O and CH_3 groups, the other is a dipole−dipole coupling interaction between the ester groups in the crystalline structure,[27−29] and yet another is crystalline packing. The interaction between the C═O and CH_3 groups may cause the low-frequency shift of the C═O stretching band. However, according to the quantum chemical calculation by Dybal et al.,[28] the magnitude of the shift is expected to be just a few wavenumbers. Thus, the interaction cannot explain the large shift by 25 cm^{-1}.

Another possible interpretation for the low-frequency shift of the crystalline band is the transition dipole coupling of the ester groups in the crystalline state.[29−31] It is well-known that for polymer systems a band splitting occurs due to the dipole−dipole coupling when the molecules form an ordered structure. According to the crystal structure of PHB revealed by X-ray crystallography,[26,27] the polymer chains form a helical structure, and the crystal lattice of the polymer contains two left-handed helical molecules in antiparallel orientation. The neighboring C═O groups along the chain are located closely in the crystal structure. Therefore, one may suppose that the dipole−dipole interaction between the C═O groups takes place in the crystalline structure, yielding the splitting of the C═O stretching band. However, this possibility is also unlikely because the spectral patterns of IR in Figure 3 are similar to those of corresponding Raman spectra obtained for the cast samples (the Raman data not shown). Usually, the dipole−dipole interaction provides quite different spectral patterns for IR and Raman spectra, so that the comparison between the IR and Raman spectra does not give the support for the idea of the dipole−dipole coupling. Consequently, we infer that the low-frequency

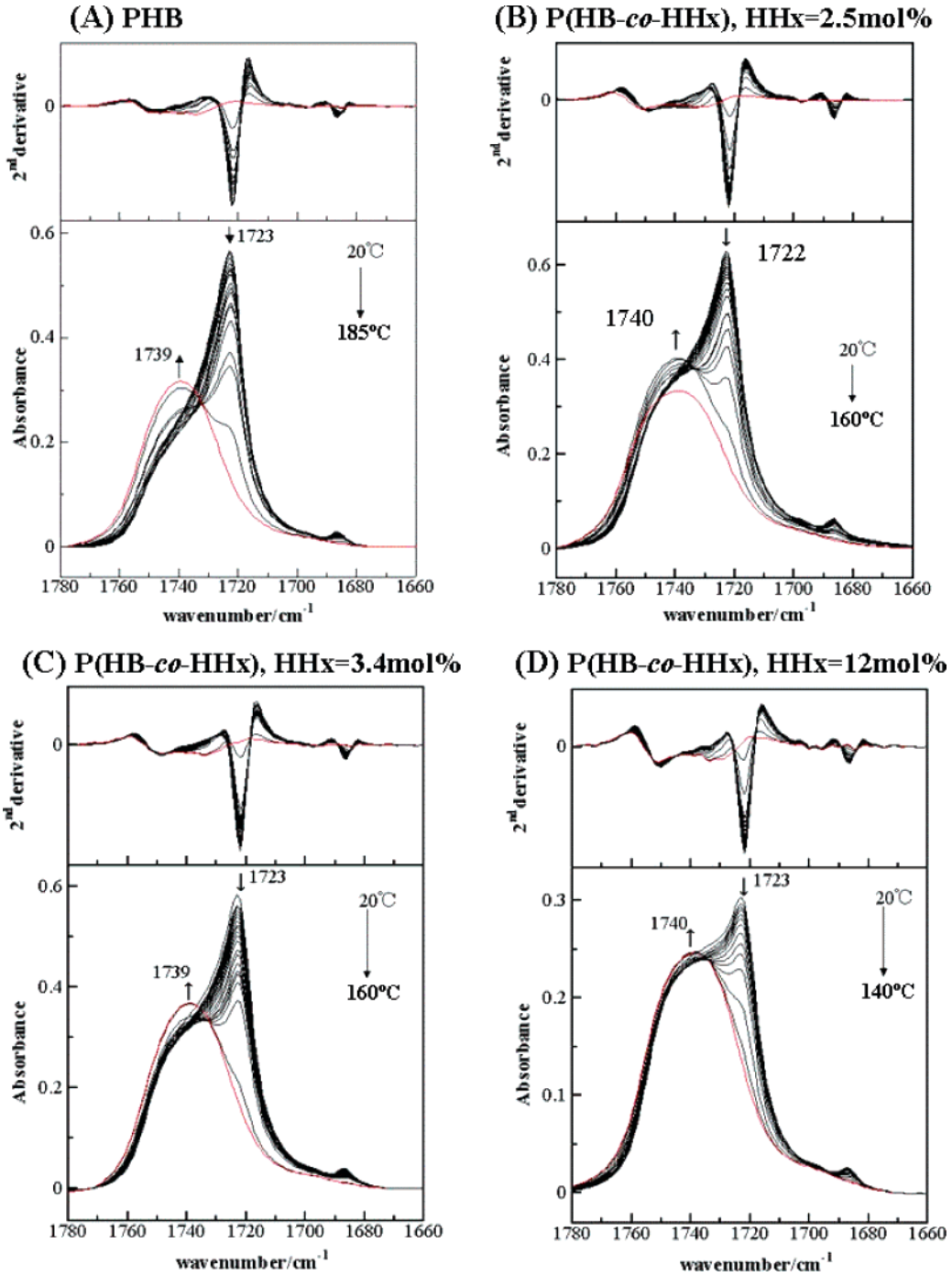

Figure 3. Temperature-dependent IR spectral variations in the C═O stretching band region of (A) PHB and P(HB-*co*-HHx) with HHx content of (B) 2.5, (C) 3.4, and (D) 12 mol %. Spectra were measured over a temperature range of 20 °C to a high temperature (PHB, 185 °C; HHx = 2.5 mol %, 160 °C; HHx = 3.4 mol %, 160 °C; HHx = 12 mol %, 140 °C). Second derivatives of the spectra are also shown on the top of each figure.

shift of the C═O stretching band is ascribed to the crystalline packing.

Comparison of IR Spectra in the C═O Stretching Band Region among PHB and P(HB-*co*-HHx) (HHx = 2.5, 3.4, and 12 mol %). It is very important to compare the IR spectra in the C═O stretching region among PHB and P(HB-*co*-HHx) (HHx = 2.5, 3.4, and 12 mol %). Of note in the comparison of the four spectra at room temperature is that the relative intensity of the broad feature centered at around 1740 cm^{-1} due to the amorphous parts increases with the increase in the HHx content. This result is in a good agreement with the fact that the order of crystallinity is PHB, P(HB-*co*-HHx) (HHx = 2.5 mol %), P(HB-*co*-HHx) (HHx = 3.4 mol %), and P(HB-*co*-HHx) (HHx = 12 mol %). Another important point in the comparison is that the frequency of the crystalline C═O band is almost identical among the four kinds of PHAs. This point will be discussed later together with the frequencies of CH_3 asymmetric stretching, C−O−C stretching, and CH_3 symmetric deformation bands.

Temperature-Dependent IR Spectral Changes in the C═O Stretching Band Region. Thermally induced alterations in the crystalline states of PHB and P(HB-*co*-HHx) (HHx = 2.5, 3.4, and 12 mol %) can be monitored by the temperature-dependent intensity varia-

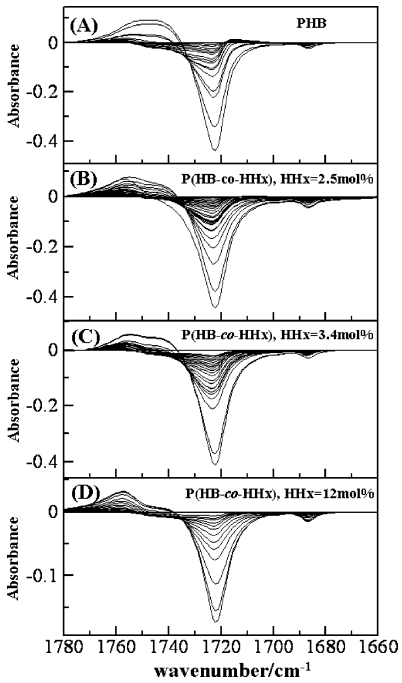

Figure 4. Difference spectra calculated from the spectra shown in Figure 3. The spectra measured at room temperature were used as reference spectra.

tion of the C═O stretching band at 1723 cm^{-1}. Figure 5 plots the normalized peak height of the band at 1723 cm^{-1} vs temperature for PHB and P(HB-*co*-HHx) (HHx = 2.5, 3.4, and 12 mol %). It can be seen from Figure 5 that the intensity of the crystalline band at 1723 cm^{-1} of PHB decreases only slightly from 20 to 160 °C and decreases markedly above 170 °C, while the intensity of the corresponding band of P(HB-*co*-HHx) (HHx = 12 mol %) starts changing from a lower temperature (60 °C). The intensity changes of the band at 1723 cm^{-1} of P(HB-*co*-HHx) (HHx = 2.5 and 3.4 mol %) are closer that of PHB than that of P(HB-*co*-HHx) (HHx = 12 mol %).

We recently studied thermal behavior of PHB and P(HB-*co*-HHx) (HHx = 12 mol %) by means of WAXD.[20] We measured the WAXD patterns of PHB and P(HB-*co*-HHx) (HHx = 12 mol %) over a temperature range from 25 °C to high temperature (PHB; 174.3 °C, P(HB-*co*-HHx) (HHx = 12 mol %); 110 °C).[20] Of particular note is that the temperature-dependent variations of the normalized peak height at 1723 cm^{-1} of PHB and P(HB-*co*-HHx) (HHx = 12 mol %) (Figure 5) are very similar to those of the (110) and (020) peak areas of their WAXD patterns. These IR results in Figure 5 reveal that the crystal structure of PHB is retained until nearly 160 °C, and above 170 °C it disappears very rapidly. The trends of thermal behavior of the crystalline structures of P(HB-*co*-HHx) (HHx = 2.5 and 3.4 mol %) are close to that of PHB, although the sharp drop of the crystalline state occurs near 150 °C for P(HB-*co*-HHx) (HHx = 2.5 and 3.4 mol %). The melting points of PHB and P(HB-*co*-HHx) (HHx = 2.5 and 3.4 mol %) revealed by DSC are respectively 170, 150, and 148 °C. Therefore, it seems that the crystalline structures of PHB and P(HB-*co*-HHx) (HHx = 2.5 and 3.4 mol %) are kept until just below the melting temperature.

Particularly striking in Figure 5 is the fact that the thermal behavior of P(HB-*co*-HHx) (HHx = 12 mol %) is clearly different from that of PHB and P(HB-*co*-HHx) (HHx = 2.5 and 3.4 mol %). It can be seen from Figure 5 that the crystalline state of P(HB-*co*-HHx) (HHx = 12 mol %) deforms gradually from about 60 °C, which is lower by 50 °C than its melting temperature. The result of the temperature-dependent changes in the WAXD patterns also indicated that the crystalline state of P(HB-*co*-HHx) (HHx = 12 mol %) starts disappearing from about 50 °C.[20] In contrast to PHB and P(HB-*co*-HHx) (HHx = 2.5 and 3.4 mol %) that show the sudden collapse in the crystalline state from just below their melting temperatures, the change in the crystalline state of P(HB-*co*-HHx) (HHx = 12 mol %) is very gradual. The HHx content in P(HB-*co*-HHx) (HHx = 12 mol %) is fairly high compared with those in the rest. Probably, the high HHx content produces a number of

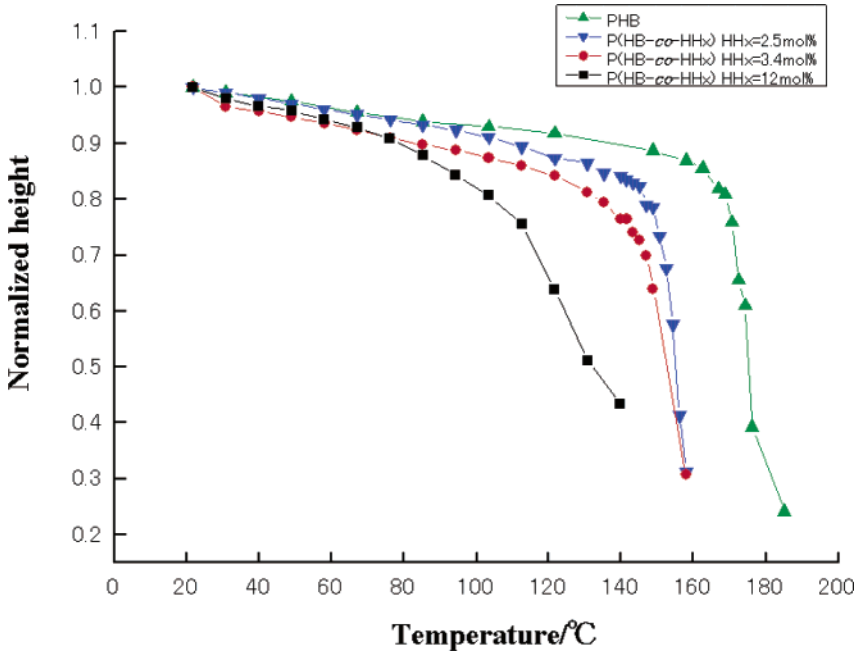

Figure 5. Plots of the normalized peak height of the C═O stretching band at 1723 cm^{-1} due to the crystalline state vs temperature for PHB and P(HB-*co*-HHx) (HHx = 2.5, 3.4, and 12 mol %).

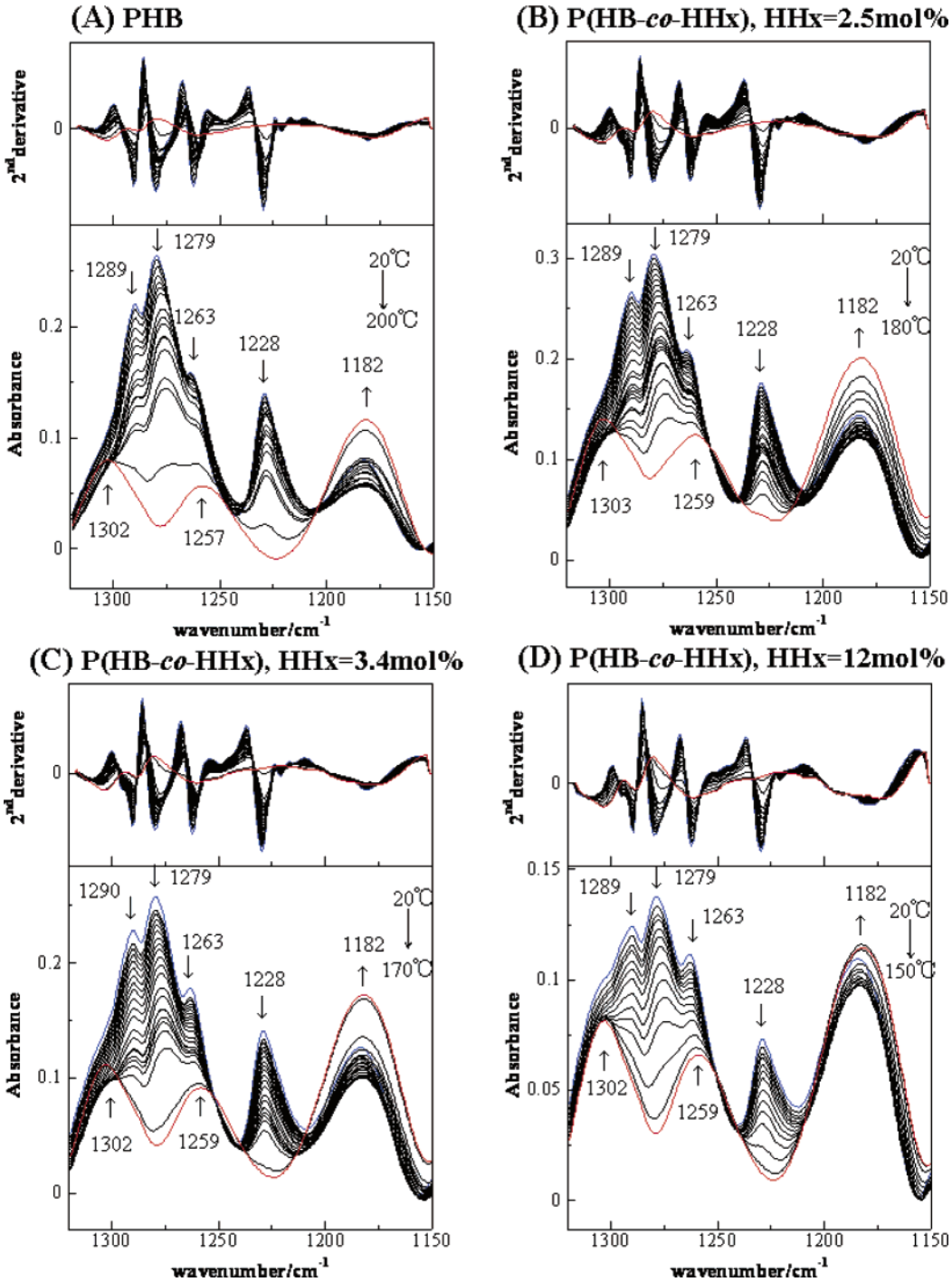

Figure 6. Temperature-dependent IR spectra variations in the C−O−C stretching band region of (A) PHB and P(HB-*co*-HHx) with HHx content of (B) 2.5, (C) 3.4, and (D) 12 mol % measured over a temperature range of 20 °C to a high temperature (PHB, 185 °C; HHx = 2.5 mol %, 160 °C; HHx = 3.4 mol %, 160 °C; HHx = 12 mol %, 140 °C). Second derivatives of the spectra are also shown on the top of each figure.

amorphous parts, leading to the significant modification of the thermal behavior of P(HB-*co*-HHx) (HHx = 12 mol %).

In our previous paper[22] on the 2D IR correlation spectroscopy study of PHB and P(HB-*co*-HHx) (HHx = 12 mol %), it was reported that the asynchronous 2D spectrum generated from the temperature-induced variations in IR spectra in the C=O stretching band region of PHB and P(HB-*co*-HHx) (HHx = 12 mol %) clearly revealed the coexistence of two crystalline bands at 1731 and 1723 cm^{-1}. The major crystalline band at 1723 cm^{-1} shares asynchronous cross-peaks with the amorphous band at 1740 cm^{-1}. This observation suggested that the melting of the crystalline structure does not simultaneously result in the formation of the completely amorphous structure. The phase transition process of PHB and P(HB-*co*-HHx) (HHx = 12 mol %) takes place through an intermediate state.[22] Shoulders of the broad band at 1723 cm^{-1} in the difference spectra in Figure 4 seem to correspond to the minor crystalline band at 1731 cm^{-1}.

−C−O−C− Stretching Band Region of IR Spectra. Temperature-dependent IR spectral variations in the C−O−C stretching band region of PHB and P(HB-*co*-HHx) (HHx = 2.5, 3.4, and 12 mol %) are shown in Figure 6. Second derivatives of the spectra are also

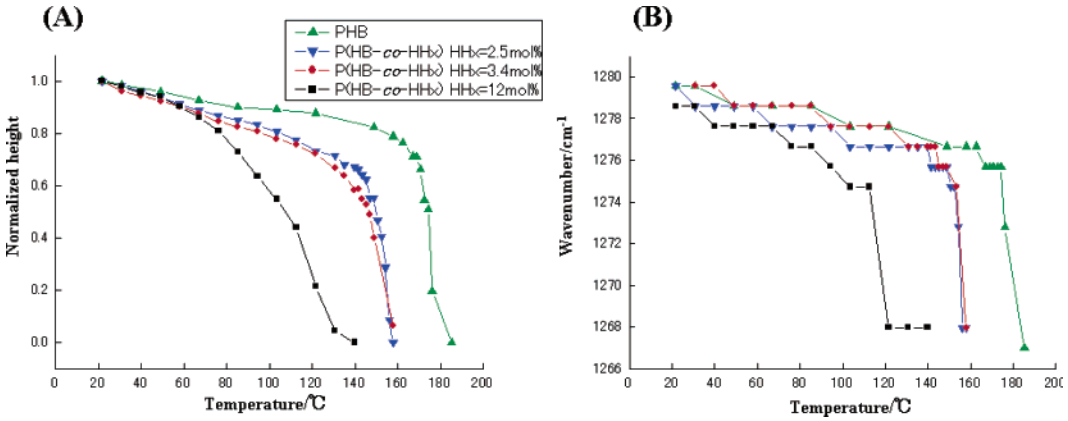

Figure 7. (A) Plots of the normalized peak height of the C−O−C stretching band at 1228 cm^{-1} due to the crystalline state vs temperature for PHB and P(HB-*co*-HHx) (HHx = 2.5, 3.4, and 12 mol %). (B) Plots of the wavenumber of the band near 1279 cm^{-1} due to the C−O−C stretching mode vs temperature for PHB and P(HB-*co*-HHx) (HHx = 2.5, 3.4, and 12 mol %).

shown on the top of each figure. In this region not only bands due to the C−O−C stretching modes but also those due to the CH and CH_2 bending modes are expected to appear,[32] and thus band assignments in this region are not straightforward. The spectra in the 1320−1150 cm^{-1} region at room temperature are dominated by four bands at 1289, 1279, 1263, 1228, and 1182 cm^{-1}, while those measured at high temperatures consist of three major features near 1302, 1257, and 1180 cm^{-1}. The four bands at 1289, 1279, 1263, and 1228 cm^{-1} do not appear in the spectra measured at high temperatures corresponding to the spectra of the amorphous states, and the bands at 1302 and 1257 cm^{-1} appear only weakly as a shoulder in the spectra at room temperature. Thus, it is very reasonable to assign bands at 1289, 1279, 1263, and 1228 cm^{-1} to the crystalline state and to attribute those at 1302 and 1257 cm^{-1} to the amorphous state. The former four bands may be due to the helical structures whereas the latter two seem to arise from the random structures. The band at 1180 cm^{-1} probably consists of two bands ascribed to the crystalline and amorphous states, respectively. The 1279 cm^{-1} band, which shows a low-frequency shift with temperature, might be due to the CH_2 wagging mode.

Of note in the comparison of Figure 6A−D is that the frequencies of the four crystalline bands are almost identical among the four kinds of PHAs, and those of the two amorphous bands are also nearly the same among them. These observations together with the observations in the C═O stretching region lead us to conclude that the helical structures of the crystalline states of the four PHAs are very similar to each other. Accordingly, the structural differences among PHB and P(HB-*co*-HHx) (HHx = 2.5, 3.4, and 12 mol %) do not lie in the structures of the crystalline states themselves but lie in the ratio between the crystalline and amorphous components. In other words, the inclusion of the HHx comonomer does not change the helical structure but destroys the helical structure from place to place, leading to the reduction of crystallinity. In the case of P(HB-*co*-HHx) (HHx = 12 mol %), the percentage of HHx is fairly high, and thus it contains a considerably high level of the amorphous parts. Therefore, the crystalline structure is easily deformed even at fairly low temperature. In contrast, the HHx content is much less for P(HB-*co*-HHx) (HHx = 2.5 and 3.4 mol %), and thus, it seems that the crystalline structures are stable until just below their melting points.

Figure 7A depicts the normalized peak height of the band near 1228 cm^{-1} due to the crystalline state vs temperature for PHB and P(HB-*co*-HHx) (HHx = 2.5, 3.4, and 12 mol %), and Figure 7B plots the wavenumber of the band near 1279 cm^{-1} vs temperature for them. It can be seen from Figure 7 that the variations in the crystalline bands at 1279 and 1228 cm^{-1} start from much lower temperature in the spectra of P(HB-*co*-HHx) (HHx = 12 mol %) than in the spectra of PHB and P(HB-*co*-HHx) (HHx = 2.5 and 3.4 mol %). These results indicate that the helical structure is destroyed even from low temperature in P(HB-*co*-HHx) (HHx = 12 mol %), while it remains up to nearly 170 °C and is suddenly collapsed at around 170 °C in PHB. The thermal behavior of P(HB-*co*-HHx) (HHx = 2.5 and 3.4 mol %) is close to that of PHB in terms of that the helical structure is retained up to high temperatures.

CH Stretching Band Region of IR Spectra. Figure 8 displays IR spectra in the 3050−2850 cm^{-1} region of PHB and P(HB-*co*-HHx) (HHx = 2.5, 3.4, and 12 mol %) measured over a temperature range of 20 °C to a higher temperature (PHB, 185 °C; HHx = 2.5 mol %, 160 °C; HHx = 3.4 mol %, 160 °C; HHx = 12 mol %, 140 °C). Their second derivatives and difference spectra in the 3030−2950 cm^{-1} are shown in Figure 9 and Figure 10, respectively. The difference spectra were calculated by using the spectra measured at room temperature as the reference spectra.

A group of bands in the 3015−2960 cm^{-1} region, those in the 2945−2925 cm^{-1} region, and those in the 2885−2865 cm^{-1} region are assigned to CH_3 asymmetric stretching modes, CH_2 antisymmetric stretching modes, and CH_3 symmetric stretching modes, respectively.[32] The original spectra, their second derivatives, and the difference spectra readily identify five bands at 3009, 2995, 2983, 2974, and 2967 cm^{-1} assignable to the CH_3 asymmetric stretching modes. Only the band at 2983 cm^{-1} increases with temperature. The difference spectra clearly demonstrate this effect (Figure 10). Therefore, the band at 2983 cm^{-1} is assigned to the CH_3 asymmetric stretching mode of the amorphous parts. The other bands at 3009, 2995, 2974, and 2967 cm^{-1} are ascribed to the CH_3 asymmetric stretching modes of the crystalline parts.

Comparison of the spectrum of PHB at 185 °C with that of P(HB-*co*-HHx) (HHx = 12 mol %) at 140 °C (Figure 8A,D) reveals that the latter shows a shoulder at 2962 cm^{-1}. Comparison of the second-derivative spectra of PHB with those of P(HB-*co*-HHx) (HHx = 12

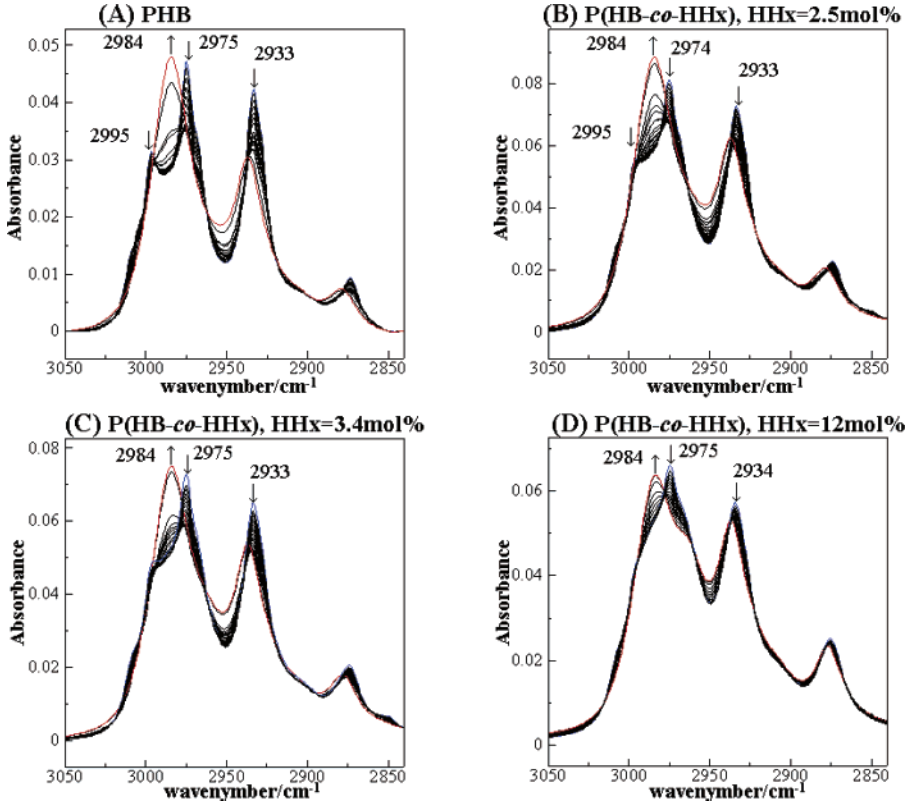

Figure 8. Temperature-dependent IR spectra variations in the CH stretching region of (A) PHB and P(HB-*co*-HHx) with HHx content of (B) 2.5, (C) 3.4, and (D) 12 mol % measured over a temperature range of 20 °C to a high temperature (PHB, 185 °C; HHx = 2.5 mol %, 160 °C; HHx = 3.4 mol %, 160 °C; HHx = 12 mol %, 140 °C).

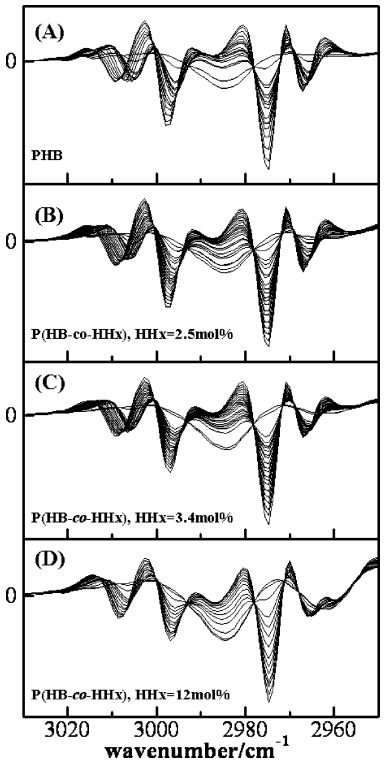

Figure 9. Second derivatives of the spectra shown in Figure 8.

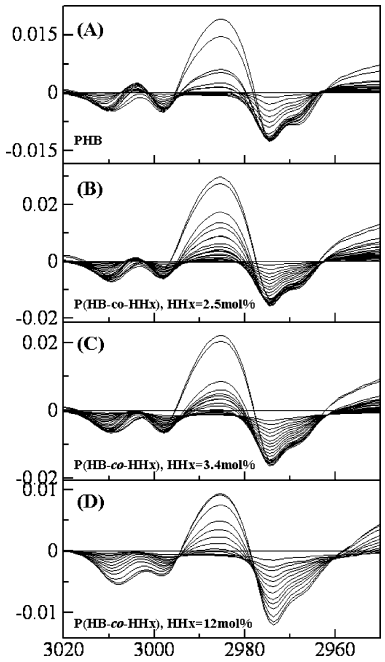

Figure 10. Difference spectra calculated from the spectra shown in Figure 8. The spectra obtained at room temperature were employed as reference spectra.

mol %) (Figure 9A,D) also shows that the former does not have the band at 2962 cm^{-1}, but the latter has it, and that its intensity changes little with temperature. Thus, the band at 2962 cm^{-1} is ascribed to the asymmetric stretching mode of the CH_3 group in the branched alkyl group. P(HB-*co*-HHx) (HHx = 2.5 and 3.4 mol %) also shows a very weak band at 2962 cm^{-1}.

C−H···O Hydrogen Bond in PHAs. It has been well-known that the CH_3 asymmetric stretching bands appear in the 2975−2950 cm^{-1} region.[32] Thus, the appearance of the CH_3 asymmetric stretching band at 3009 cm^{-1} is rather unusual. Recently, several research groups reported that the appearance of a CH_3 asym-

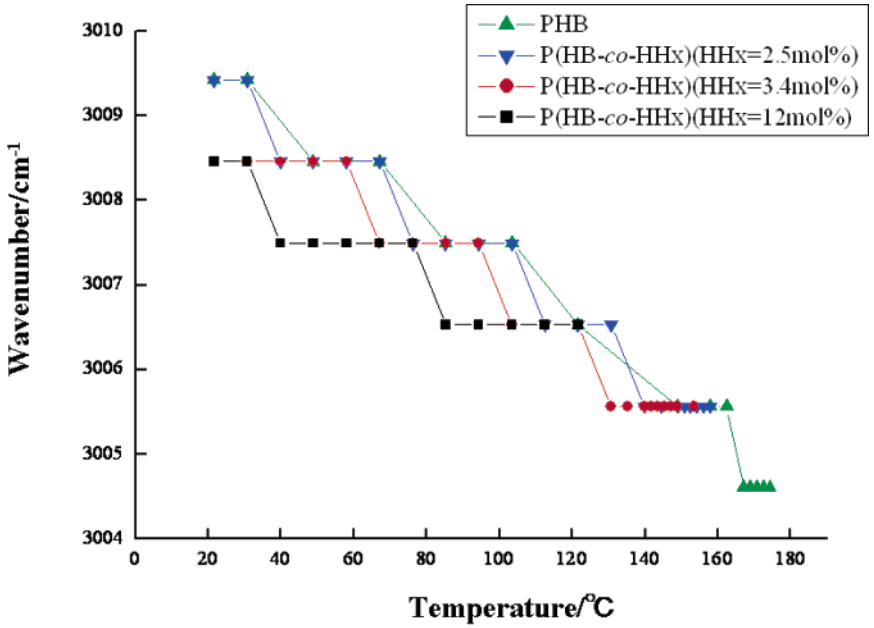

Figure 11. Temperature-dependent changes in the wavenumber of the CH stretching band at 3009 cm^{-1} of PHB and P(HB-*co*-HHx) (HHx = 2.5, 3.4, and 12 mol %).

metric stretching band above 3000 cm^{-1} indicates the possibility of a C−H···O hydrogen bond.[24,25,33−36] For example, Matsuura et al.[34] reported that 1-methoxy-2-(dimethylamino)ethane shows a CH_3 asymmetric stretching band at 3016.5 cm^{-1} and discussed about the C−H···O interaction between the O atom of the CH_3O-$CH_2CH_2N(CH_3)_2$ and the H atom of the (N)CH_3. The C−H···O interaction has recently been recognized a kind of weak hydrogen bond.[23−25] Vibrational spectroscopy and quantum chemical calculations have been used extensively to explore the nature of such weak hydrogen bonds. In contrast to usual hydrogen bonds involving an OH or NH group, the higher the frequency of a CH stretching band, the stronger the C−H···O hydrogen bond.[34−40] It is still unclear why the C−H bond becomes short when the C−H···O hydrogen bond becomes strong. However, there are many experimental and theoretical evidences for the high-frequency shift of the CH stretching band for the stronger C−H···O bond. Thus, the appearance of the CH_3 asymmetric stretching band at 3009 cm^{-1} leads us to conclude that the C═O group is interacting with the CH_3 group in the four PHAs. This conclusion may be supported by the fact that the distance between the O atom of the C═O group and the H atom of the one of the three CH bonds of the CH_3 group can be significantly shorter than the van der Waals separation. Judging from the frequency, the C−H···O interaction is rather weak, and its strength is very similar among the four polymers. According to the crystal structure of PHB revealed by X-ray crystallography,[26,27] the crystal lattice of the polymer contains two left-handed helical molecules in two antiparallel orientation (Figure 2A). It is also found in the crystal structure that the CH_3 group in one helical structure and the C═O group in the other helical structure are in close proximity, and there is a pair of such proximity between the CH_3 group and the C═O group (Figure 2). Therefore, it seems that a chain of C−H···O hydrogen bond pairs link the two helical structures in the antiparallel orientation.

According to the quantum chemical calculation, the bonding energy of C−H···O hydrogen bonds in 1-methoxy-2-(methylthio)ethane ($CH_3OCH_2CH_2SCH_3$), 1,2-dimethoxyethane ($CH_3OCH_2CH_2OCH_3$), 1-methoxy-2-(dimethylamino)ethane ($CH_3OCH_2CH_2N(CH_3)_2$), and 2-(methylseleno)ethanol ($HOCH_2CH_2SeCH_3$) is 4−6 kJ/mol.[35] The CH_3 asymmetric stretching band of CH_3-$OCH_2CH_2SCH_3$ appears at 3018 cm^{-1},[34] while that of the four polymers is identified at 3009 cm^{-1}. Moreover, the distance between the H atom and the O atom in the C−H···O bond is 2.55 Å for $CH_3OCH_2CH_2N(CH_3)_2$[35] and 2.63 Å for PHB. Therefore, the bonding energy of C−H···O hydrogen bonds in the PHAs seems to be less than 4 kJ/mol. However, judging for the heat of fusion of the PHAs investigated (∼12.5 kJ/mol[41]), the C−H···O hydrogen bond plays an important role in stabilizing the helical structure. In $CH_3OCH_2CH_2SCH_3$, CH_3OCH_2-CH_2OCH_3, $CH_3OCH_2CH_2N(CH_3)_2$, and $HOCH_2CH_2$-$SeCH_3$, an electronegative atom such as oxygen, sulfur, nitrogen, or selenium atom is bonded directly to the carbon atom of the CH_3 group that is involved in the C−H···O interaction. On the other hand, in PHB and P(HB-*co*-HHx) (HHx = 2.5, 3.4, and 12 mol %) instead of an electronegative atom, the carbon atom is bonded directly to the CH_3 group that is interacting with the C═O group. It is well-known that the C−H···O hydrogen bond becomes stronger when an electronegative atom is bonded to the CH_3 group that is involved in the C−H···O interaction.[23−25] Therefore, the present result for PHB and P(HB-*co*-HHx) is in good agreement with this general rule.

Thus far, we have called the 3009 cm^{-1} band the CH_3 asymmetric stretching band. However, strictly speaking, this is incorrect because one of the three C−H bonds of the CH_3 group is involved in the C−H···O interaction while the rest is free. Probably, we should simply call it the C−H stretching band. The CH_3 group that is involved in the C−H···O hydrogen bond should give one C−H stretching band and two pseudo CH_2 stretching bands, one antisymmetric and one symmetric stretching bands.[35] The bands at 2995, 2974, and 2967 cm^{-1} may be due to the pseudo CH_2 stretching bands.

Figure 11 illustrates temperature-dependent variations of the wavenumber of the CH stretching band near

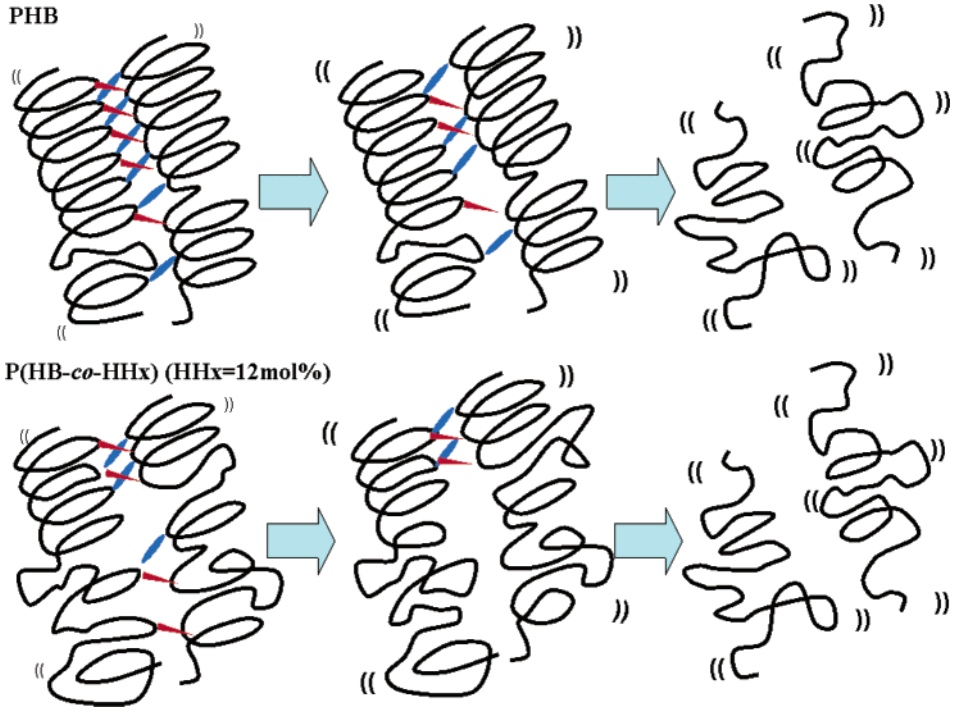

Figure 12. A proposed model for parallel helical structures linked by a chain of C−H···O hydrogen bond pair and their thermal deformation process.

3009 cm^{-1} for PHB and P(HB-*co*-HHx) (HHx = 2.5, 3.4, and 12 mol %). Interestingly, the CH stretching band shows a temperature-dependent wavenumber shift. These shifts of the CH band indicate the changes in the strength of the C−H···O hydrogen bonds. The profiles of the temperature-dependent variations of the frequency of the CH stretching band (Figure 11) are quite different from those of the temperature-dependent changes in the C═O stretching band at 1723 cm^{-1} (Figure 5) and the two bands at 1228 and 1279 cm^{-1} (Figure 7). The frequencies of the CH stretching band start changing even from 30 °C and continue varying gradually for all the polymers investigated, while the spectral changes in the C═O stretching, and C−O−C stretching vibration regions begin at much higher temperatures. The frequency shift in the CH stretching region reflects the variation in the C−H···O hydrogen bond, while the spectral alterations in the other regions are sensitive to the deformation of the helical structures. Therefore, it is very likely that the C−H···O hydrogen bond becomes gradually weak just above room temperature, leading eventually to the collapse of the helical structures in the crystal parts of the PHAs (Figure 12).

Conclusion

The present study has aimed at exploring the structure and thermal behavior of PHB and three new types of bacterial copolyesters, P(HB-*co*-HHx) (HHx = 2.5, 3.4, and 12 mol %) by means of IR spectroscopy. The four polymer samples have very similar chemical structures but have different contents of HHx from 0 to 12 mol %. By comparing the IR spectra among the four kinds of polymers and by analyzing their temperature-dependent IR spectra using the second-derivative spectra and the difference spectra, we have been able to make band assignments in the C−H stretching, C═O stretching, and C−O−C stretching band regions and to classify bands in the three regions into the crystalline bands and the amorphous bands. The anomalous high frequencies of CH_3 stretching bands have suggested that existence of the C−H···O hydrogen bonds in the PHAs investigated. Comparison of the temperature-dependent IR spectra variations of the four kinds of polymers has allowed us to compare their thermal behavior. In other words, the effects of the addition of HHx group on the thermal behavior, the helical structure, and the C−H···O interaction can be investigated.

The following conclusions can be reached from the present study.

1. The calculation of the distance between the O atom of the C═O group in one helix structure and the H atom of one of the three C−H bonds of the CH_3 group in the other helix structure from the X-ray crystallographic data of PHB has shown that the distance is 2.63 Å, which is shorter than the sum of the van der Waals separation (2.72 Å). This result and the appearance of the CH_3 asymmetric stretching band at 3009 cm^{-1} suggest that there is a C−H···O hydrogen bond between the CH_3 group and the C═O group in the four PHAs investigated. It is likely that a chain of C−H···O bonds pair combine the two parallel helical structures. Figure 12 illustrates it. The bonding energy of the C−H···O hydrogen bond has been estimated to be less than 4 kJ/mol. Compared with the heat of fusion (12.5 kJ/mol) of PHB, it is not small.

2. The temperature-dependent changes in the intensity of the crystalline C═O stretching band at 1723 cm^{-1}, those in the intensities and wavenumbers of the bands at 1227 and 1273 cm^{-1}, and those in the wavenumber of the CH_3 symmetric deformation band at 1378 cm^{-1} reflect the deformation of the helical structure, while the temperature-dependent low wavenumber shift of the CH_3 asymmetric band at 3009 cm^{-1} indicates the weakening of the C−H···O interaction. The present study has clearly revealed that the weakening of CH···O hydrogen bond proceeds gradually even from low temperature, and the deformation of helical structure takes

place after the weakening of the C−H···O hydrogen bond advances to some extent (Figure 12).

3. The CH stretching bands at 3009, 2995, 2974, and 2967 cm^{-1}, the C═O stretching band at 1723 cm^{-1}, and the bands at 1287, 1279, 1263, and 1228 cm^{-1} are ascribed to the crystalline states. The frequencies of these bands are almost identical among the four PHAs, indicating that the helical structure, and the nature and strength of the C−H···O hydrogen bond are almost identical among the four kinds of PHAs. Therefore, it seems that the HHx comonomer does not modify the helical structures, probably because the HHx comonomers are located mainly in the amorphous parts.

4. The changes in the helical structure start from fairly low temperature and proceed gradually in P(HB-*co*-HHx) (HHx = 12 mol %). In contrast, the changes occur rather suddenly just below the melting temperatures in PHB and P(HB-*co*-HHx) (HHx = 2.5 and 3.4 mol %). P(HB-*co*-HHx) (HHx = 12 mol %) contains much larger amounts of the HHx comonomers and thus much larger amounts of amorphous parts. Thus, it seems that the helical structures are cut down in many places in P(HB-*co*-HHx) (HHx = 12 mol %), and therefore, the helical structures are easily broken even at fairly low temperature.

Acknowledgment. The authors thank Prof. H. Matsuura (Graduate School of Science, Hiroshima University), Dr. J. Dybal (Institute of Macromolecular Chemistry, Academy of Sciences of the Czech Republic, Czech Republic), Prof. L. Bokobza (Laboratoire PCSM, ESPCI, France), Dr. T. Tanaka (Graduate School of Science and Technology, Kobe University, Japan), Associate Prof. H. Yamaguchi (School of Science and Technology, Kwansei Gakuin University, Japan), and Dr. K. Ishii (Kaneka Corp., Japan) for valuable discussions.

References and Notes

(1) Doi, Y. *Microbial Polyesters*; VCH Publishers: New York, 1990.
(2) Anderson, A. J.; Dawes, E. A. *Microbiol. Rev.* **1990**, *54*, 450.
(3) Lundgren, D. G.; Alper, R.; Schnaitman, C.; Marchessault, R. H. *J. Bacteriol.* **1965**, *89*, 245.
(4) Dawes, E. A. *Novel Biodegradable Microbial Polymers*; Kluwer Academic: Dordrecht, 1990.
(5) Lara, L. M.; Gjalt, W. H. *Microbiol. Mol. Biol. Rev.* **1991**, *63*, 21.
(6) Iwata, T.; Doi, Y. *Macromol. Chem. Phys.* **1999**, *200*, 2429.
(7) Satkowski, M. M.; Melik, D. H,; Autran, J.-P.; Green, P. R.; Noda, I.; Schechtman, L. A. In *Biopolymers*, Steinbüchel, A., Doi, Y., Eds.; Wiley-VCH: Weinheim, 2001; p 231.
(8) Yoshie, N.; Menju, H.; Sato, H.; Inoue, Y. *Macromolecules* **1995**, *28*, 6516.
(9) Doi, Y.; Kitamura, S.; Abe, H. *Macromolecules* **1995**, *28*, 4822.
(10) Web site: www.nodax.com.
(11) Abe, H.; Doi, Y.; Aoki, H.; Akehata, T. *Macromolecules* **1998**, *31*, 1791.
(12) Kobayashi, G.; Shiotani, T.; Shima, Y.; Doi, Y. In *Biodegradable Plastics and Polymers;* Doi, Y., Fukuda, K., Eds.; Elsevier: Amsterdam, 1994; p 410.
(13) Kunioka, M.; Tamaki, A.; Doi, Y. *Macromolecules* **1989**, *22*, 694.
(14) Shimamura, E.; Kasuya, K.; Kobayashi, G.; Shiotani, T.; Shima, Y.; Doi, Y. *Macromolecules* **1994**, *27*, 878.
(15) Kobayashi, G.; Shiotani, T.; Shima, Y.; Doi, Y. *Stud. Polym. Sci.* **1994**, *12*, 410.
(16) Xu, J.; Guo, B.; Yang, R.; Wu, Q.; Chen, G.; Zhang, Z. *Polymer* **2002**, *43*, 6893.
(17) Yoshie, N.; Asaka, A.; Yazawa, K.; Kuroda, Y.; Inoue, Y. *Polymer* **2003**, *44*, 7405.
(18) Wu, Q.; Tain, G.; Sun, S.; Noda, I.: Chen, G.-Q. *J. Appl. Polym. Sci.* **2001**, *82*, 934.
(19) Tain, G.; Wu, Q.; Sun, S.; Noda, I.; Chen, G.-Q. *Appl. Spectrosc.* **2001**, *55*, 888.
(20) Sato, H.; Nakamura, M.; Padermshoke, A.; Yamaguchi, H.; Terauchi, H.; Ekgasit, S.; Noda, I.; Ozaki, Y. *Macromolecules* **2004**, *37*, 3763.
(21) Sato, H.; Padermshoke, A.; Nakamura, M.; Murakami, R.; Hirose, F.; Senda, K.; Terauchi, H.; Ekgasit, S.; Noda, I.; Ozaki, Y. *Macromol. Symp.*, in press.
(22) Padermshoke, A.; Sato, H.; Katsumoto, Y.; Ekgasit, S.; Noda, I.; Ozaki, Y. *Vib. Spectrosc.*, in press.
(23) Desiraju, G. R.; Steiner, T. *The Weak Hydrogen Bond*; Oxford University Press: New York, 1999.
(24) Scheiner, S. In *Advances in Molecular Structure Research*; Hargittai, M., Hargittai, I., Eds.; JAI Press: Stamford, CT, 2000; Vol. 6, pp 159−207.
(25) Hobza, P.; Havlas, Z. *Chem. Rev.* **2000**, *100*, 4253.
(26) Yokouchi, M.; Chatani, Y.; Tadokoro, H.; Teranishi, K.; Tani, H. *Polymer* **1973**, *14*, 267.
(27) Cornibert, J.; Marchessault, H. R. *J. Mol. Biol.* **1972**, *71*, 735.
(28) Dybal, J.; Sato, H.; Ozak, Y., to be published.
(29) Dybal, J.; Schneider, B. *Spectrochim. Acta, A* **1985**, *41*, 691.
(30) Dybal, J.; Spevacek, J.; Schneider, B. *J. Polym. Sci., Part B: Polym. Phys.* **1986**, *24*, 657.
(31) Galbiati, E.; Zoppo, M. D.; Tieghi, G.; Zerbi, G. *Polymer* **1993**, *34*, 1806.
(32) Colthup. N. B.; Daly, L. H.; Wiberley, S. E. *Introduction to Infrared and Raman Spectroscopy*, 3rd ed.; Academic Press: New York, 1990; p 215.
(33) Gu, Y.; Kar, T.; Scheiner, S. *J. Am. Chem. Soc.* **1999**, *121*, 9411.
(34) Matsuura, H.; Yoshida, H.; Hieda, M.; Yamanaka, S.; Harada, T.; Shin-ya, K.; Ohno, K. *J. Am. Chem. Soc.* **2003**, *125*, 13910.
(35) Harada, T.; Yoshida, H.; Ohno, K.; Matsuura, H. *Chem. Phys. Lett.* **2002**, *362*, 453.
(36) Boldeskul, I. E.; Tsymbal, I. F.; Ryltsev, E. V.; Latajka, Z.; Barnes, A. J. *J. Mol. Struct.* **1997**, *436/437*, 167.
(37) Yoshida, H.; Harada, T.; Murase, T.; Ohno, K.; Matsuura, H. *J. Phys. Chem. A* **1997**, *101*, 1731.
(38) van der Velen, B. J.; Herrebout, W. A.; Szostak, R.; Shchepkin, D. N.; Havlas, Z.; Hobza, P. *J. Am. Chem. Soc.* **2001**, *123*, 12290.
(39) Delanoye, S. N.; Herrebout, W. A.; van der Velen, B. J. *J. Am. Chem. Soc.* **2002**, *124*, 11854.
(40) Blatchford, M. A.; Raveendran, P.; Wallen, S. L. *J. Am. Chem. Soc.* **2001**, *124*, 14818.
(41) Noda, I.; Marchessault, H. R.; Terada, M. *Polymer Data Handbook*; Oxford University Press: New York, 1999; pp 586−597.

MA049117O